ACS EARTH AND SPACE CHEMISTRY

Article

Cite This: ACS Earth Space Chem. 2019, 3, 895−904

http://pubs.acs.org/journal/aesccq

# Effects of Rare Earth Elements' Physicochemical Properties on Their Stabilization during the $Fe(II)_{aq}$-induced Phase Transformation of Ferrihydrite

Jian Hua,[†,‡] Chengshuai Liu,[*,‡,⊥] Fangbai Li,[†] Zhenke Zhu,[§] Zhiqi Wei,[†] Manjia Chen,[†] Ting Gao,[‡] and Guohong Qiu[∥]

[†]Guangdong Key Laboratory of Integrated Agro-environmental Pollution Control and Management, Guangdong Institute of Eco-Environmental Sciences & Technology, Guangzhou 510650, China

[‡]State Key Laboratory of Environmental Geochemistry, Institute of Geochemistry, Chinese Academy of Sciences, Guiyang 550081, China

[§]Key Laboratory of Agro-Ecological Processes in Subtropical Region, Institute of Subtropical Agriculture, Chinese Academy of Sciences, Changsha 410125, China

[∥]College of Resources and Environment, Huazhong Agricultural University, Wuhan 430070, China

[⊥]CAS Center for Excellence in Quaternary Science and Global Change, Xi'an 710061, China

Downloaded via CHENGDU DOCUM AND INFO CTR on September 11, 2020 at 01:41:01 (UTC).
See https://pubs.acs.org/sharingguidelines for options on how to legitimately share published articles.

**ABSTRACT:** Ferrihydrite (FHY), a widespread Fe(III) (hydr)oxide, is abundant in earth surface and critical in affecting the environmental behavior of soil elements, such as rare earth elements (henceforth referred to REEs). Under anoxic conditions, the coexisting Fe(II) induces FHY conversion to the minerals with high crystallinity, such as lepidocrocite, goethite, or magnetite, where the phase transformation processes were affected by the coexisting ions. The interactions between REE ions (henceforth referred to Ln(III)) and FHY in the transformation system, however, are still not well understood. We therefore investigated $Fe(II)_{aq}$-induced FHY transformation affected by four kinds of Ln(III) ($Ce^{3+}$, $Nd^{3+}$, $Tb^{3+}$, and $Lu^{3+}$). The discernible inhibition was found among the different treatments with different Ln(III), and both the FHY transformation and Fe atom exchange ratios decreased with coexistent Ln(III) that have larger atomic number. In this study, the Fe atom exchange ratios with different coexistent Ln(III) were linearly negatively depended on the molar enthalpy values of Ln(III), which are explained by the molar enthalpy considered to be important in affecting the adsorption behaviors of Ln(III). Furthermore, the adsorption behaviors can affect the incorporation efficiency of the Ln(III), so as to affect the Fe atom exchange and FHY phase transformation. The Ln(III) with larger atomic number can be stabilized more, which results from the effects of incompatible REEs in determining the efficiency of immobilizing Ln(III) in the transformed iron (hydr)oxides. Our research suggested the important role of FHY in the distribution of REEs and the key properties of REEs in affecting their different distribution characteristics in earth surface environments.

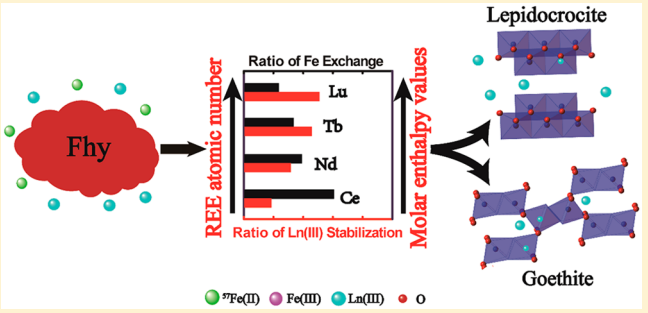


**KEYWORDS:** *Iron mineral, phase transformation, REEs, immobilization, molar enthalpy*

## 1. INTRODUCTION

Ferrihydrite (FHY) is the first type of iron (hydr)oxide during the iron mineralization in environments,[1−4] and it has been widely observed in mine waste and acidic mine drainage environments.[5−7] In comparison with the crystalline iron minerals, FHY is metastable and poorly crystalline[4,8,9] and can be easily converted to the iron (hydr)oxides with high crystallinity, like goethite and hematite, in environments.[10,11] Because of the small particle size, large surface area, and high reaction activity, FHY has been recognized as an important scavenger for a multiple of elements in environments.[4,12] Therefore, FHY is critical in contamination retention in environments.

The FHY phase transformation is more distinct than other iron (hydr)oxide in environments. $Fe(II)_{aq}$ can be oxidized into Fe(III) and then precipitate as "reactive" FHY after the continuing adsorption of $Fe(II)_{aq}$ on the FHY, then it would be transformed to goethite and lepidocrocite phases.[13,14] The Fe atom exchange and electron transfer (ETAE) have been considered as a main driving force in the iron oxides

Special Issue: Iron Redox Chemistry and Its Environmental Impact

Received: December 12, 2018
Revised: April 30, 2019
Accepted: May 8, 2019
Published: May 8, 2019


© 2019 American Chemical Society

DOI: 10.1021/acsearthspacechem.8b00201
ACS Earth Space Chem. 2019, 3, 895−904

recrystallization induced by $Fe(II)_{aq}$.[15−17] The environmental behavior of metallic elements affected by the FHY transformation, via adsorption, enwrapping, and substitution, as well as metallic ions would also affect the phase transformation process.[18,19] Considering the significant varying conditions of FHY transformation, it is important for us to understand the secondary mineral forming processes, so as to predicate the movement of contaminative element and the reactivity of iron pool in natural environment.

Rare earth elements (REEs) are referred to group 3 of the Periodic Table. The lanthanide family of REEs was constituted from La with atomic numbers from 57 to Lu with atomic numbers from 71. The mean content of REEs is relatively high in the Earth's upper crust.[20−22] REEs are commonly classified as heavy REEs (Gd−Lu) and light REEs (La−Eu) according to an opposite direction of 4f electron spin after Gd.[23] The iron (hydr)oxides of colloid and sediment significantly affect the geochemical behavior of REEs, such as stabilization, transport, and fractionation, in natural environments.[24,25] Fe- and Mn-(hydr)oxides have been reported to enrich heavy REEs, while clay colloids tend to enrich light REEs.[26,27] Thereby, the processes of FHY formation and transformation impose an important effect on the REEs' geochemical behavior in environment.[28−31]

The decreased REE's ionic radii from $La^{3+}$ (103 pm) to $Lu^{3+}$ (86 pm) was related with their increase of atomic number. The REEs with small ionic radii can facilely substitute the other main metal cations in minerals due to their equivalent ionic radii.[32,33] Quinn et al. reported that the molar enthalpies for Ln(III) sorption on amorphous ferric hydroxide increase with the increase of REE atomic number, which imposed a significant effect on the stability of Ln(III).[34] REEs are incompatible elements (total distribution coefficient $D < 1$), which lead to their visible fractionation during the process of mineral partial melting.[23,35] The physicochemical properties of REEs are considered to be the most important factors that affect their environmental behavior in environments.[36] Although the effects of REEs and the stabilization of REEs during the FHY phase transformation have been reported,[37] the most critical physicochemical properties of REEs that affected the phase transformation processes and the stabilization of REEs, as far as we know, still remained unclosed.

Therefore, four kinds of Ln(III) ($Ce^{3+}$, $Nd^{3+}$, $Tb^{3+}$, and $Lu^{3+}$) were selected for investigating the distribution of these REE ions in this study. We characterized the constituents of formed secondary minerals by XRD, for discussing the effects of different Ln(III) on the transformational products of FHY. The relative quantities of formed secondary minerals are analyzed by Rietveld quantitative analysis using powder XRD patterns. We detail the changes of Fe atom exchange, and the immobilization efficiencies of Ln(III), via analyzing the compositions of four stable Fe isotopes and the concentrations of Ln(III) in dissolved, adsorbed, and structural fraction. This research focused on the disparities of varying REE stabilization by considering their differing physicochemical properties. The results are expected to help us understand the geochemical behavior of REEs in earth surface, especially the Fe-enriched REE mining area.

## 2. MATERIALS AND METHODS

**2.1. Preparation and Characterization of FHY.** The laboratory-synthetic FHY was prepared according the previous reports.[12,38] Briefly, a 0.08 g/L of $Fe(NO_3)_3$ solution was obtained in water (MQ water) first, and the solution's pH value was titrated to pH 7−8. After sequential agitation, the resulting suspension was aged at room temperature for 6−7 h. Afterward, the suspension was decanted into several 15 mL centrifuge tubes, then centrifuged and washed with MQ water for 6−7 times. After being freeze-dried, the X-ray diffraction (XRD) of the powders was performed on a Bruker D8 advance diffractometer (Bruker Corporation, Billerica, MA, USA), operating with Cu−K$\alpha$ radiation at 40 mA and 40 kV at room temperature, for demonstrating the FHY phase. Additionally, the fresh FHY was stored at 4 °C and used for the batch experiments within 3 days.

The formed secondary minerals in the transformation experiment were collected inside the anoxic chamber (93% $N_2$, 7% $H_2$) (Coy, Grass Lake, MI, USA). The crystal phases of the formed secondary minerals was also characterized by XRD. To quantitatively determine the composition of the formed secondary minerals, the total patter solution (TOPAS) program was employed for the Rietveld quantitative analysis via adding the standard reference. The details of the analytic methods were reported in previous research.[39]

The morphological characterizations of the formed secondary minerals were analyzed with transmission electron microscopy (TEM) (Philips-CM12, FEI, Hillsboro, USA). The powdery samples were prepared according to a previous method.[12] After that, the TEM data were obtained with the dried Cu grids at 200 kV.

**2.2. Experiments of FHY Phase Transformation Induced by $Fe(II)_{aq}$.** The total batch experiments were conducted in the anoxic chamber. The $O_2$ concentration inside the anoxic chamber was maintained to less than 1 ppm by palladium catalysts. Additionally, all liquids were purged with high-purity $N_2$ (>99.999% pure) before being transferred into the anoxic chamber. After that, 48 h were needed to equilibrate the anoxic condition with the anaerobic atmosphere. The stock solution of $^{57}Fe(II)$ was prepared inside the anoxic chamber, 5 M HCl was used to dissolve the enriched $^{57}Fe(0)$ (Isoflex, $^{57}Fe$ > 96%) metal, then the enriched $^{57}Fe(II)$ solution was diluted to 100 mM. Ln(III) solutions (100 mM) were prepared with their corresponding chloride salts being dissolved inside the anoxic chamber.

Inside the anoxic chamber, each reactor of 15 mL plastic tube contained 20 mM FHY and 0 or 1 mM Fe(II) with 0 or 1 mM Ln(III). The 1,4-piperazinediethanesulfonic acid (PIPES) was used as the buffer reagent with KBr as the background electrolyte.[40] pH values of reaction suspensions were adjusted to around 7.0 before the reaction. Significantly, the additive order of reagents followed FHY, buffer solution, Ln(III), and Fe(II). The reactors were sealed with Teflon-coated butyl rubber stoppers and crimp seals after all of the chemicals were added, then covered with Al foil and placed on the rotator. Afterward, sampling was done with triplicate centrifuge tubes at specified time points (0, 2, 5, 15, 30, and 60 days) for needed analyses.

First, the 15 mL reactors were transferred outside of the anoxic chamber and centrifuged at 9500 rpm for 10 min. The 0.22 $\mu$m filters (Millipore, Burlington, MA, USA) were used to filter the resulting supernatant inside the anoxic chamber. The filtrate was acidified by adding 50 $\mu$L of concentrated HCl and referred to as dissolved fraction for analysis of the concentrations of Ln(II) and $Fe(II)_{aq}$ and the isotopic composition of $Fe_{aq}$. The 0.4 M HCl (10 mL) was used to disperse remaining solid, then the centrifuge tubes were placed


DOI: 10.1021/acsearthspacechem.8b00201
ACS Earth Space Chem. 2019, 3, 895−904

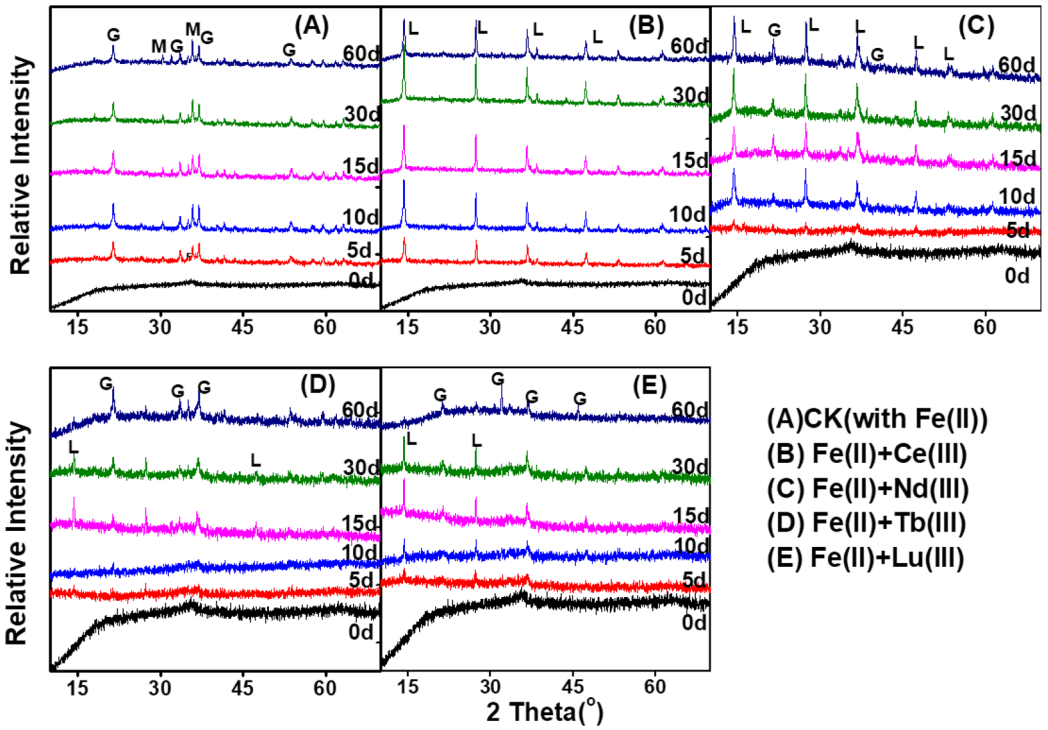


**Figure 1.** X-ray diffraction (XRD) patterns of the FHY transformation products induced by $Fe(II)_{aq}$ in different treatments with (A) no Ln(III) (CK treatment); (B) Ce(III); (C) Nd(III); (D) Tb(III); and (E) Lu(III). Experimental conditions: $[Fe(II)_{aq}]$ = 2 mM, [FHY] = 2 g/L, pH of 7.0 buffered by 25 mM 1,4-piperazinediethanesulfonic acid (PIPES)/KBr.

on the rotator for 10 min. The extractive supernatant was referred to as adsorbed fraction for analysis of the adsorbed Fe(II) ($Fe(II)_{exter}$) and Ln(III) ($Ln(III)_{exter}$).[18,41,42] At length, the remaining solid was completely dissolved in concentrated HCl. The concentrated HCl extract were referred to as structural fraction for analysis of the residual Fe ($Fe_{solid}$) and Ln(III) ($Ln(III)_{solid}$). Another batch experiment was performed in the same way in which the solid was collected for phase analysis after the suspension was centrifuged and filtered removing the supernatant.

**2.3. Determinations of Fe Isotope Compositions and the Different Species Concentrations of Fe and Ln(III).** To determine the Fe(II) and Fe(III) concentration, the Fe(II)-selective reagent ferrozine was used in this study.[43] The Ln(III) concentrations were analyzed on an inductively coupled plasma optical emission spectrometry (ICP-OES, PerkinElmer Optima 8000, Waltham, MA, USA). The iron isotopic fractions were determined on an inductively coupled plasma mass spectrometry (ICP-MS, PerkinElmer NexION 300D, Waltham, MA, USA). The details of analytical procedures were consistent with those previously described.[37]

After measuring the total counts over all four channels (i.e., $^{54}Fe$, $^{56}Fe$, $^{57}Fe$ and $^{58}Fe$), each isotope channel was divided by the sum of the total counts to obtain the iron isotope fractions ($f$). Then, the iron atom exchange percentages in the solids were calculated according to the following equation:[44,45]

$$\text{Fe atom exchange (\%)} = \frac{N_{aq}(f^{i}_{aq} - f^{t}_{Fe(II)})}{N^{Tot}_{Fh}(f^{t}_{Fe(II)} - f^{i}_{Fh})} \times 100 \quad (1)$$

where $N_{aq}$ is the moles of $Fe(II)_{aq}$ in the solution, $N^{Tot}_{Fh}$ is the total moles of Fe in the solids, $f^{i}_{aq}$ is the initial isotopic fractions of $Fe(II)_{aq}$, $f^{i}_{Fh}$ is the initial isotopic fractions of FHY, and $f^{t}_{Fe(II)}$ is the isotopic fraction of $Fe(II)_{aq}$ at the reaction time of $t$.

## 3. RESULTS

**3.1. $Fe(II)_{aq}$-induced Phase Transformation of FHY Affected by Different Ln(III).** The constituents of formed secondary minerals during the FHY phase transformation induced by $Fe(II)_{aq}$ were determined using XRD (Figure 1). The results indicated the varying effects of different Ln(III) on FHY phase transformation rates and pathways in the system. In the control treatment without Fe(II) and Ln(III), there was no discernible phase transformation of FHY throughout the studied reaction time (data not shown). In the treatment with Fe(II) (CK), however, an efficient phase transformation of FHY was observed (Figure 1A), in which a number of FHY were transformed to goethite and magnetite after 60 days of incubation. In the treatments with Ln(III) ($Ce^{3+}$, $Nd^{3+}$, $Tb^{3+}$, and $Lu^{3+}$), the phase transformation pathway of FHY were changed. FHY were transformed to lepidocrocite phase first, and then some formed lepidocrocite was further transformed to goethite, in which no magnetite was detected all through the experimental period (Figure 1). The phase transformation pathway of FHY induced by $Fe(II)_{aq}$ was changed with different Ln(III). In the light Ln(III) (Ce(III) and Nd(III)) treatments, FHY was converted to lepidocrocite. Goethite phase was found at 10 days in the Nd(III) treatments, while no goethite phase was formed in Ce(III) treatment. In the heavy Ln(III) (Tb(III) and Lu(III)) treatments, FHY were converted to lepidocrocite and goethite, and goethite phase was the only product at the end of the incubation.

To further study the effects of different Ln(III) on the FHY transformation with the coexistence of $Fe(II)_{aq}$, the phase compositions of formed products in different treatments were



DOI: 10.1021/acsearthspacechem.8b00201
ACS Earth Space Chem. 2019, 3, 895−904

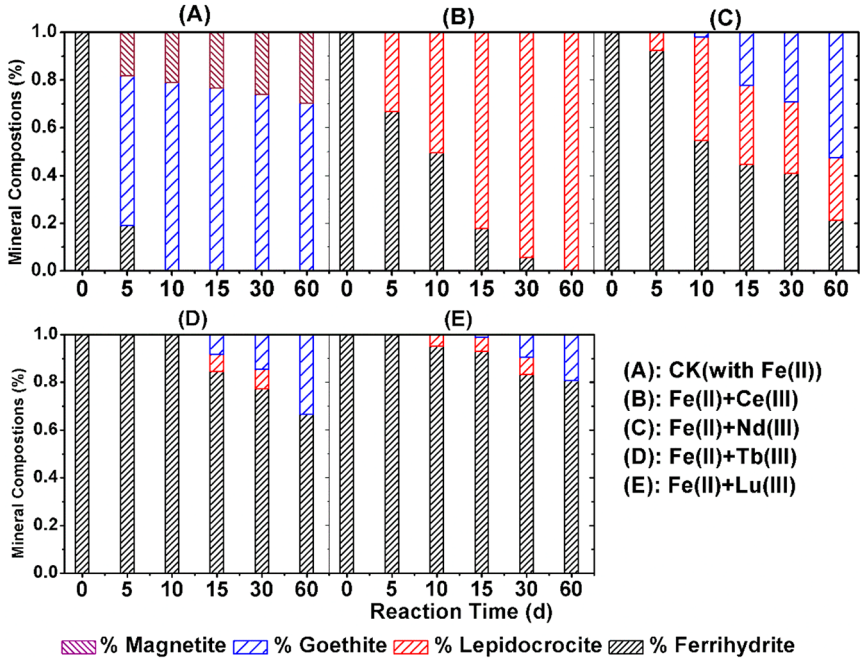


**Figure 2.** Temporal changes of the compositions of formed secondary minerals during the $Fe(II)_{aq}$-induced FHY transformation in different treatments with (A) no Ln(III) (CK treatment); (B) Ce(III); (C) Nd(III); (D) Tb(III); and (E) Lu(III). The same experimental conditions are provided in Figure 1.

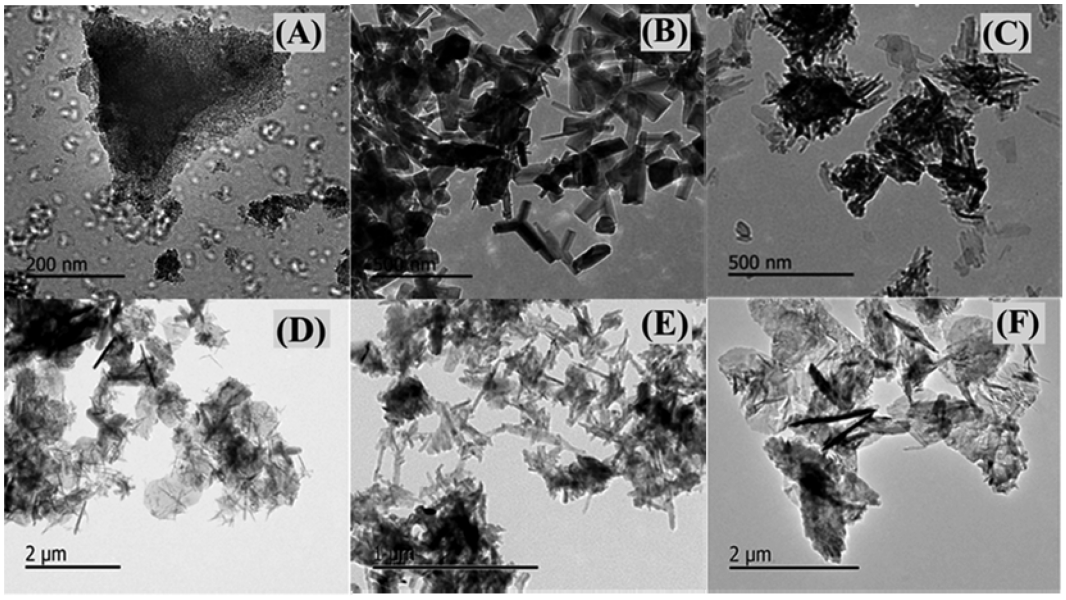


**Figure 3.** Transmission electron microscope (TEM) images of transformed products after the $Fe(II)_{aq}$-induced FHY transformation reaction for 60 days in different treatments with (A) FHY (before reaction); (B) no Ln(III) (CK treatment); (C) Ce(III); (D) Nd(III); (E) Tb(III); and (F) Lu(III).

quantitatively analyzed, the details of the analytical method were discussed above. Figure 2 shows the changes of relative quantities of secondary minerals in the transformational products. The quantitative results of formed secondary minerals indicate that the coexistent Ln(III) inhibited the phase transformation of FHY. In the CK treatment only with Fe(II), the relative quantity of goethite and magnetite was 18.2% and 62.3% after incubation for 5 days, and the composition of FHY was gradually decreased and completely disappeared after 10 days. At the beginning of the incubation (5 days), magnetite was formed in the CK treatment, and then the magnetite composition increased following the decrease of goethite. In the treatment with Ce(III), FHY was converted to lepidocrocite throughout the duration of the experiments. In the treatment with Nd(III), parts of FHY were converted to lepidocrocite first and then to goethite at 10 days, and the relative quantities of FHY, goethite, and lepidocrocite were 21.2%, 26.2%, and 52.6%, respectively, at the end of incubation (60 days). In the treatment with Tb(III) and Lu(III), little FHY was converted to lepidocrocite and goethite, in which the compositions of goethite increased and lepidocrocite decreased during the incubation. The relative FHY and goethite were


DOI: 10.1021/acsearthspacechem.8b00201
ACS Earth Space Chem. 2019, 3, 895−904

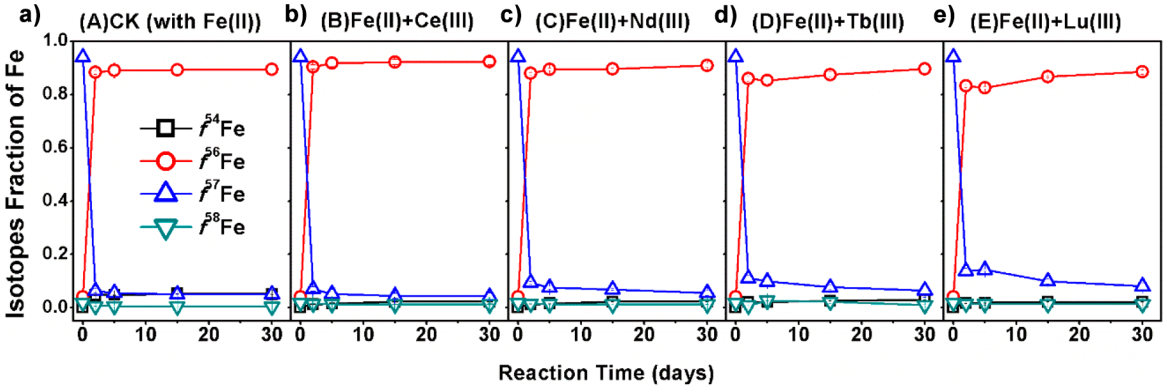


**Figure 4.** Temporal changes of four Fe isotopic compositions in aqueous solution during the $Fe(II)_{aq}$-induced FHY transformation in different treatments with (A) no Ln(III) (CK treatment); (B) Ce(III); (C) Nd(III); (D) Tb(III); and (E) Lu(III). Experimental conditions: $[Fe(II)_{aq}]$ = 2 mM, [FHY] = 2 g/L, pH of 7.0 buffered by 25 mM 1,4-piperazinediethanesulfonic acid (PIPES)/KBr.

66.5% and 33.5% in Tb(III) treatment, while 80.6% and 19.4% in Lu(III) treatment, respectively. No magnetite was formed in all Ln(III) treatments.

The TEM images for the obtained solid at the end of reaction with or without Ln(III) also indicate the significant disparities among the mineral morphologies of the transformational products (Figure 3). The star-shaped particles could be found in the CK treatment (Figure 3B), which indicated the formation of goethite and magnetite in a high crystallinity. The lath-shaped lepidocrocite and acicular goethite were detected in the Ce(III) and Nd(III) treatment (Figure 3C,D). Goethite can also be observed in Nd(III), Tb(III), and Lu(III) treatments (Figure 3E,F).

**3.2. Effects of Ln(III) on ETAE between FHY and $Fe(II)_{aq}$.** To explore the influencing mechanism of Ln(III) on the process of FHY phase transformation, the quantitatively Fe atom exchanges were studied through reacting 1 mM $^{57}Fe$ labeled $Fe(II)_{aq}$ with 20 mM FHY in natural Fe isotope composition abundance at pH 7.0 with the coexistence of different Ln(III). The four stable Fe isotope compositions ($f^nFe$) changed in dissolved, adsorbed, and residual fractions, which were used to calculate the Fe atom exchange ratio with eq 1.

The $f^{57}Fe$ in the dissolved fraction decreased rapidly at the beginning of the reaction, then continually decreased in subsequent days slowly (Figure 4). Simultaneously, the $f^{56}Fe$ in the dissolved fraction increased rapidly, but then continually increased on subsequent days slowly. Conversely, the $f^{57}Fe$ in residual fraction slightly increased and $f^{56}Fe$ decreased slowly at the first stage of the reaction, then remained approximately constant. Compared with the Tb(III) and Lu(III) treatments, the extents of change of $f^{57}Fe$ and $f^{56}Fe$ in both dissolved and residual fractions in Ce(III) and Nd(III) treatments were discernibly larger.

The results of Fe atom exchange ratios are shown in Figure 5. It should be noted that the recrystallized fraction of the solids could be calculated by homogeneous model, due to the continuous re-equilibration between the solid and the fluid.[46] Although the distributions of phases (ferrihydrite, lepidocrocite, and goethite) were not homogeneous in our system, in the study, the all Fe(III) (hydr)oxides in a treatment were considered as a holistic Fe(III) phase. The coexisting Ln(III) resulted in the disparities of exchange efficiency between the holistic Fe(III) phase and $Fe(II)_{aq}$ in different Ln(III) treatment. Then the eq 1 was utilized in the relative context

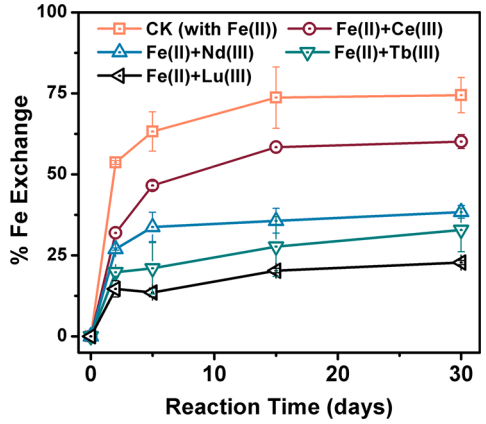


**Figure 5.** Temporal changes of Fe atom exchange ratios during the $Fe(II)_{aq}$-induced transformation of FHY in different treatments with the same experimental conditions provided in Figure 4.

for comparison of different treatments as demonstrated previously,[47,48] which can wholly reflect the effects of different Ln(III) on the iron atom exchange ratios in this study with different treatments.

The ratios gradually increased in the all treatments during the first few days. In the CK treatment only with Fe(II), the Fe atom exchange ratio reached 75% over 30 days. The Ln(III) presence totally decreased the Fe atom exchange ratios although with different extents with different Ln(III). In the treatment with light Ln(III), including Ce and Nd, the ratios were decreased to 60% and 38%, respectively. In the treatments with heavy Ln(III), including Tb and Lu, the ratios were further decreased to 33% and 23%, respectively. The above results clearly suggest the inhibited Fe atom exchange by the coexistent Ln(III) in the transformation experiment, and in comparison, the heavy Ln(III) inhibited more than light Ln(III).

**3.3. Ln(III) Species Distribution During the FHY Transformation Induced by $Fe(II)_{aq}$.** Previous studies suggest that FHY transformation induced by $Fe(II)_{aq}$ can incorporate the adsorbed metal ions into the structure of formed secondary minerals. The processes involving the metal ions with higher binding abilities resulted in larger stabilized amounts of metal ions in the formed products.[19] To explore the distribution behavior of Ln(III) during the FHY phase transformation, the concentrations of Ln(III) in dissolved,


DOI: 10.1021/acsearthspacechem.8b00201
ACS Earth Space Chem. 2019, 3, 895−904

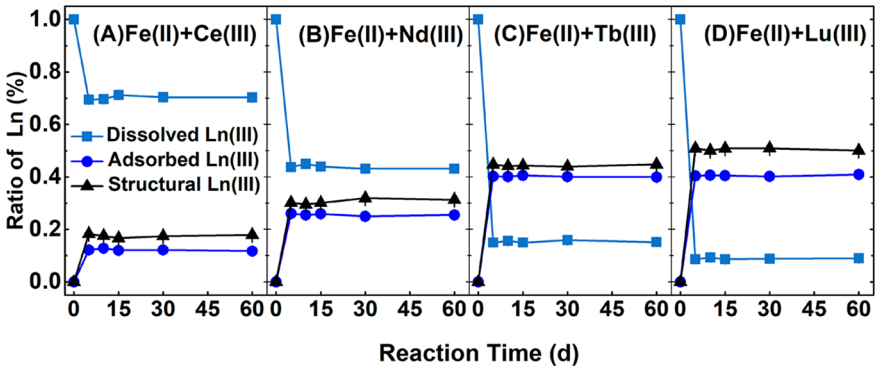


**Figure 6.** Temporal changes of the ratio of different Ln(III) species during the $Fe(II)_{aq}$-induced phase transformation of FHY in the presence (A) Ce(III), (B) Nd(III), (C) Tb(III), and (D) Lu(III).

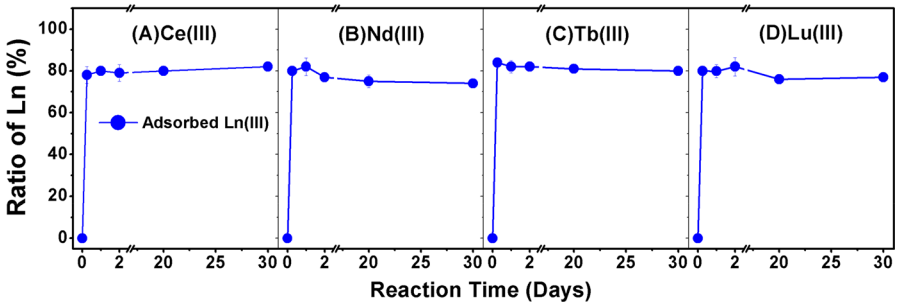


**Figure 7.** Temporal ratio changes of different Ln(III) species during adsorption on FHY: (A) Ce(III), (B) Nd(III), (C) Tb(III), and (D) Lu(III).

adsorbed, and structural fraction were studied; the results were shown in Figure 6. Except for the prominent changes during the 5 days of incubation, the concentrations of the different Ln(III) remain constant throughout the studied reaction time. In comparison, the stabilized heavy Ln(III) percentages were higher than light Ln(III) during the FHY phase transformation. In the treatment with Ce(III), 12% of Ce(III) was adsorbed on the surface and 17% of Ce(III) was incorporated into the formed secondary minerals. In the treatment with Nd(III), approximately 25% of Nb(III) was adsorbed on the surface of solid and 30% of Nd(III) was structurally stabilized by the formed products. In the treatment with Tb(III), approximately 40% of Tb(III) was adsorbed on the surface of solid and 45% of Tb(III) incorporated into the secondary formed minerals. In comparison, approximately 41% of Lu(III) was adsorbed on the surface of solid and 50% of Lu(III) was incorporated into the formed secondary minerals. In the comparative controls without $Fe(II)_{aq}$, the coexistent Ln(III) sharply adsorbed on the surface of FHY in a few hours. After that, the reaction system reached the adsorption equilibrium gradually (Figure 7). Additionally, we did not detect any phase transformation when without $Fe(II)_{aq}$.

## 4. DISCUSSION

**4.1. $Fe(II)_{aq}$-induced Phase Transformation of FHY Affected by Different Ln(III).** Previous studies indicated that metal ions can obviously affect the transformation processes of FHY in the system, which was ascribed to the disparities of physicochemical properties, such as ionic strength, ion radii, and binding ability.[19,49,50] The metal ions with high binding affinity can inhibit the ETAE, so as to change the FHY phase transformation rates and products, in which the binding ability of metal ions imposed negative effects on the FHY phase transformation.[19,51] Compared with chalcophile or siderophile elements, REEs are lithophile elements and considered to be more facile to combine with oxygen.[23] The specific physicochemical properties of REEs are expected to pose important effects on the FHY phase transformation in the study.

XRD and TEM results clearly manifested the different effects of different Ln(III) on the formed secondary mineral products in the transformation experiment. In CK treatment, FHY was converted to goethite and magnetite; while in the Ln(III) treatments, the decreased percentages of FHY transformation followed the increase of REE atomic number. Furthermore, the ratios of Fe atom exchange decreased as the REE atomic number increased in the treatments with Ln(III). The competition of Fe(II) with coexisting ions for the surface adsorption on iron (hydr)oxides would be crucial to the iron (hydr)oxide transformation.[45,52] The more Fe(II) adsorbed on FHY surface, the more iron atom exchange obtained and, consequently, the more efficient the FHY transformation.[19,53]

The strong adsorption of Ln(III) in comparative controls without $Fe(II)_{aq}$ indicated that the coexistent Ln(III) played a critical role in inhibiting the FHY transformation in the experiment (Figure 7). The FHY phase transformation rates were correlated with the binding constants of metals with FHY as demonstrated previously.[19] In this study, however, the disparate inhibition effects of different Ln(III) on the FHY phase transformation cannot be simply ascribed to the binding constants for Ln(III), because the binding constants of Ln(III) are highly differentiated from previously studied heavy metal ions.

The physicochemical properties of Ln(III), such as the molar enthalpy values, imposed important effects on the behavior of adsorbed Ln(III) and further affected the FHY phase transformation and Ln(III) stabilization in the reaction systems when with Ln(III). The positive adsorption enthalpy


DOI: 10.1021/acsearthspacechem.8b00201
ACS Earth Space Chem. 2019, 3, 895−904

suggests that the adsorption capability of the coexisting ion was strengthened.[54] In the present study, the positive adsorption enthalpy impeded oriented attachment of formed secondary minerals due to the surface charge variation of the particles. In addition, the positive adsorption enthalpy plays a critical role in accelerating the Ln(III) incorporation into the secondary formed minerals. The disparate inhibition of Fe atom exchange and the FHY phase transformation, therefore, were explained from the positive molar enthalpy values of Ln(III). The potential explanations were explored in this study, including the adsorption behavior of Ln(III), the incorporation of Ln(III), and the oriented attachment of particles.

Quinn et al. calculated the molar enthalpy values for Ln(III) adsorption on amorphous ferric hydroxide based on a surface complexation model.[34] Generally, the chemical adsorption is often exothermal, which means the molar enthalpy values are less than 0.[55] However, the calculated molar enthalpy values of Ln(III) adsorption on the amorphous ferric hydroxide were greater than 0, and the molar enthalpy values for Ln(III) sorption increased with the increase of REE atomic number.[34] These results indicate that the adsorption behavior of Ln(III) on FHY was significantly different from other metal ions, so as to affect the Fe atom exchange and FHY phase transformation.

Compared with light Ln(III), the molar enthalpy values of heavy Ln(III) increased more distinctly. As we know, the behaviors of the coexistent metal ions always played a critical role in affecting iron oxide transformation with the coexistence of $Fe(II)_{aq}$.[18,19] The previous study indicated that the structural incorporation of metal cations can inhibit the Fe atom exchange.[56] The adsorption behaviors of metal ions influenced the incorporation efficiency of the metal ions during $Fe(II)_{aq}$-induced transformation of iron (hydr)oxides, which further affected the Fe atom exchange.[18,19,56] Additionally, the disparities of the molar enthalpy indicated that the adsorption behaviors of different Ln(III) were differentiated.[34] Therefore, the molar enthalpy values were considered to be important in influencing the Fe atom exchange ratios and FHY phase transformation in the study.

The linearly negative relationship between Fe atom exchange ratios and the molar enthalpy values for Ln(III) adsorption on amorphous ferric hydroxide can be found, as Figure 8 shows (the data of La(III) and Ho(III) are quoted from ref 37). Previous studies indicated that the surface interactions with the species (e.g., organic matter and Si) would decrease the attachment and formation efficiencies of larger crystals.[57−59] The previous study has reported the key role of oriented aggregation growth in influencing the phase transformation at low temperature.[60] Furthermore, when the reaction pH conditions were close to the point-of-zero charge ($pH_{PZC}$) of the solid phases, the oriented aggregation growth can be accelerated.[59,61] The adsorption of Ln(III) changed the surface charge of the phases,[62,63] so as to impede the formation of larger crystals. Therefore, the lower Fe atom exchange ratios obtained with Ln(III) in higher molar enthalpy values were ascribed to the surface charge variation, which inhibited the attachment and formation of larger crystals via impeding the oriented aggregation growth.[58,59,63]

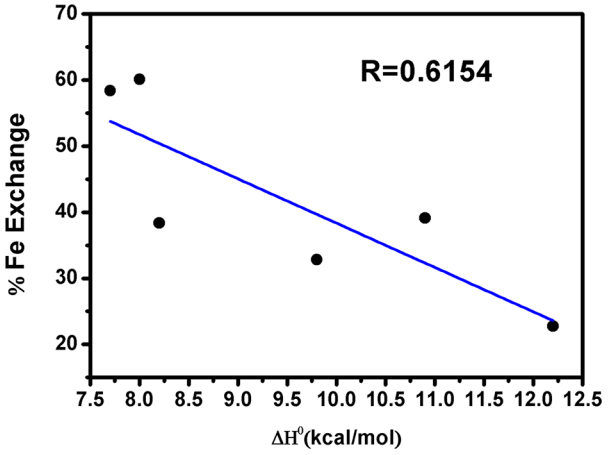


**Figure 8.** Relationship between the Fe atom exchange ratios and the molar enthalpy values of Ln(III) adsorption on FHY (the data of La(III) and Ho(III) are from ref 37).

### 4.2. Different Stabilization Behavior of Different Ln(III) during FHY Transformation Induced by $Fe(II)_{aq}$.

The iron (hydr)oxides transformation induced by $Fe(II)_{aq}$, especially FHY, was reported to be efficient in immobilizing the coexisting metals.[64,65] REEs, such as Nd and Lu, could be incorporated into the mineral structure by isomorphous replacement and lattice enwrapping during the transformation.[19,65−67] Here, the lattice enwrapping means the atoms of Ln(III) are incorporated into vacancies of pores in the transformed minerals.[68,69] FHY, because of the large surface area, has been confirmed to be more effective at adsorbing Ln(III) on the surface than other iron (hydr)oxides. In our experiments, the reaction systems reached the adsorption equilibrium over 2 days. The ratio of adsorbed Ln(III) sharply increased in the first 2 days, and vice versa, the ratios of dissolved Ln(III) species sharply decreased. After that, the ratio changes of the Ln(III) gradually diminished because of the system's adsorption equilibrium, although the phase transformation and the Fe atom exchange still occurs. Additionally, the stabilization and release of Ln(III) synchronized since the Ln(III) were incorporated into the structure of solid phases in the early stage of the reaction.[18,70] Consequently, the stabilization efficiency of Ln(III) species gradually decreased in the later stages. Therefore, the temporal ratio changes of different Ln(III) species were negligible (Figure 6).

In addition, our results clearly indicated that the percentages of stabilized heavy Ln(III) were more than light Ln(III), and the distribution of Ln(III) in the treatment with varying Ln(III) were different. During the FHY transformation induced by $Fe(II)_{aq}$, the adsorbed and structural Ln(III) increased with the increase of REE atomic number (Figure 6). As previously reported, Cr(III) was more easily substituted into iron (hydr)oxides because of the similar ionic radius between Cr(III) and Fe(III).[18,71] The stabilized amounts of Ln(III) increased with the increase of REE atomic number, which can be explained from ionic radius decreases and was closer to that of Fe(III) across the trend of light to heavy REE.[37] Additionally, the charge and the chemical bond were considered to be important in affecting the substituted efficiency of the coexistent ions too. The ionic radius, charge, and chemical bond also have been confirmed to be important in affecting the compatibility of REE in rock-forming mineral melts.[35,36,72] The comprehensive effect of those factors affected the substituted efficiency of REE significantly. Therefore, the compatibility of REE was considered to be important in inhibiting Fe atom exchange and phase transformation in the experiment.



DOI: 10.1021/acsearthspacechem.8b00201
ACS Earth Space Chem. 2019, 3, 895−904

Compared with the more incompatible elements, the less incompatible elements are easier to be incorporated into the structure minerals.[35,73] For the four studied Ln(III), the incompatible extent decreases with the increase of REE atomic number,[23,71,73] thereby more Ln(III) were stabilized as the structural species for the heavy Ln(III) (Tb(III) and Lu(III)) with higher atomic number. The results of the relationship between stabilizing Ln(III) percentages and the molar enthalpy for Ln(III) adsorption was linearly positive. Considering the Ln(III) with high molar enthalpy values inhibited the phase transformation of FHY more, the Ln(III) could be more facilely stabilized into the FHY phase than the formed secondary phase through possible enwrapping, substitution, or coprecipitation. Overall, the percentages of stabilized Ln(III) increased for the Ln(III) with larger atomic number during the FHY phase transformation induced by $Fe(II)_{aq}$.

## 5. CONCLUSIONS

FHY is a remarkable absorbent for stabilizing metal ions in soils because its low crystallinity and small particle size. The physicochemical properties of REEs can significantly influence the efficiency and pathways of the FHY transformation in this study. The coexistent Ln(III) inhibited the rates and products of phase transformation of FHY, and the inhibition efficiencies were different with different Ln(III). The adsorption behaviors of Ln(III) influenced the incorporation efficiency and phase transformation rate during the FHY transformation with the coexistence of $Fe(II)_{aq}$. The molar enthalpy values of Ln(III) imposed important effects on the adsorption behavior of Ln(III), which further influence the phase transformation rates and Fe atom exchange. The physicochemical properties of different Ln(III) also affect the stabilization of Ln(III) during the phase transformation processes. The immobilization efficiencies of different Ln(III) followed the descending order of the percentages of Ln(III) incompatible in Ce < Nd < Tb < Lu. The results were due to less incompatible elements that are easier to be incorporated into the structure minerals. We expect these findings are significant for assessing the key factors that affect the mobility and transfer behavior of Ln(III) in earth surface, especially the Fe-enriched REE mining area.

## AUTHOR INFORMATION


### Corresponding Author

*E-mail: liuchengshuai@vip.gyig.ac.cn.

### ORCID

Chengshuai Liu: 0000-0003-0133-0119

Fangbai Li: 0000-0001-9027-9313

Guohong Qiu: 0000-0002-1181-3707


### Notes

The authors declare no competing financial interest.

## ACKNOWLEDGMENTS

The authors thank the financial supports from the National Natural Science Foundations of China (U1701241, 41673135, and U1612442); the Frontier Science Research Programme of the Chinese Academy of Sciences (CAS) (QYZDB-SSW-DQC046); the National Key Research and Development Program of China (2018YFD080041); the Science and Technology Planning Project of Guangdong Province, China (2016TX03Z086 and 2016B020242006); the Science and Technology Planning Project of Guangzhou, China (201710010128 and 201804020037); and the Hundred Talents Program of CAS.

## REFERENCES


(1) Schwertmann, U.; Fischer, W. R. Natural "amorphous" ferric hydroxide. *Geoderma* **1973**, *10* (3), 237−247.

(2) Carlson, L.; Schwertmann, U. Natural ferrihydrites in surface deposits from Finland and their association with silica. *Geochim. Cosmochim. Acta* **1981**, *45* (3), 421−429.

(3) Schwertmann, U.; Friedl, J.; Stanjek, H. From Fe(III) ions to ferrihydrite and then to hematite. *J. Colloid Interface Sci.* **1999**, *209* (1), 215−223.

(4) Cornell, R. M.; Schwertmann, U. *The Irrn Oxides: Structure, Properties, Reactions, Occurrences and Uses*; Wiley-VCH, 2003.

(5) Carlson, L.; Bigham, J. M.; Schwertmann, U.; Kyek, A.; Wagner, F. Scavenging of As from acid mine drainage by schwertmannite and ferrihydrite: a comparison with synthetic analogues. *Environ. Sci. Technol.* **2002**, *36* (8), 1712−1219.

(6) Moldovan, B. J.; Jiang, D. T.; Hendry, M. J. Mineralogical characterization of arsenic in uranium mine tailings precipitated from iron-rich hydrometallurgical solutions. *Environ. Sci. Technol.* **2003**, *37* (5), 873−879.

(7) Lalonde, K.; Mucci, A.; Quellet, A.; Gélinas, Y. Preservation of organic matter in sediments promoted by iron. *Nature* **2012**, *483* (7388), 198−200.

(8) Manceau, A.; Combes, J. M. Structure of Mn and Fe oxides and oxyhydroxides: A topological approach by EXAFS. *Phys. Chem. Miner.* **1988**, *15* (3), 283−295.

(9) Manceau, A. Local Structure of ferrihydrite and feroxyhite by EXAFS spectroscopy. *Clay Minerals* **1993**, *28* (2), 165−184.

(10) Cudennec, Y.; Lecerf, A. The transformation of ferrihydrite into goethite or hematite, revisited. *J. Solid State Chem.* **2006**, *179* (3), 716−722.

(11) Xiao, W.; Jones, A. M.; Li, X.; Collons, R. N.; Waite, T. D. Effect of shewanella oneidensis on the kinetics of Fe(II)-catalyzed transformation of ferrihydrite to crystalline iron oxides. *Environ. Sci. Technol.* **2018**, *52* (1), 114−123.

(12) Schwertmann, U.; Cornell, R. M. Iron oxides in the laboratory: preparation and characterization, 2nd, completely revised and enlarged edition. *Mineralogical Magazine* **2000**, *61* (408), 740−741.

(13) Boland, D. D.; Collins, R. N.; Miller, C. J.; Glover, C. J.; Waite, T. D. Effect of solution and solid-phase conditions on the Fe(II)-accelerated transformation of ferrihydrite to lepidocrocite and goethite. *Environ. Sci. Technol.* **2014**, *48* (10), 5477−5485.

(14) Jones, A. M.; Murphy, C. A.; Waite, T. D.; Collins, R. N. Fe(II) interactions with smectites: temporal changes in redox reactivity and the formation of green rust. *Environ. Sci. Technol.* **2017**, *51* (21), 12573−12582.

(15) Williams, A. G.; Scherer, M. M. Spectroscopic evidence for Fe (II)− Fe (III) electron transfer at the iron oxide− water interface. *Environ. Sci. Technol.* **2004**, *38* (18), 4782−4790.

(16) Katz, J. E.; Zhang, X.; Attenkofer, K.; Chapman, K. W.; Frandsen, C.; Zarzycki, P.; Rosso, K. M.; Falcone, R. W.; Waychunas, G. A.; Gilbert, B. Electron small polarons and their mobility in iron (oxyhydr)oxide nanoparticles. *Science* **2012**, *337* (6099), 1200−1203.

(17) Reddy, T. R.; Reddy, T. R.; Frierdich, A. J.; Beard, B. L.; Johnson, C. M. The effect of pH on stable iron isotope exchange and fractionation between aqueous Fe(II) and goethite. *Chem. Geol.* **2015**, *397*, 118−127.

(18) Frierdich, A. J.; Scherer, M. M.; Bachman, J. E.; Engelhard, M. H.; Rapponotti, B. W.; Catalano, J. G. Inhibition of trace element release during Fe (II)-activated recrystallization of Al-, Cr-, and Sn-substituted goethite and hematite. *Environ. Sci. Technol.* **2012**, *46* (18), 10031−10039.

(19) Liu, C.; Zhu, Z.; Li, F.; Liu, X.; Liao, Z.; Lee, J.; Shih, K.; Tao, L.; Wu, D. Fe(II)-induced phase transformation of ferrihydrite: The inhibition effects and stabilization of divalent metal cations. *Chem. Geol.* **2016**, *44*, 110−119.




DOI: 10.1021/acsearthspacechem.8b00201
*ACS Earth Space Chem.* 2019, 3, 895−904

(20) Taylor, S. R.; Mclennan, S. M. The continental crust: Its composition and evolution, an examination of the geochemical record preserved in sedimentary rocks. *Journal of Geology* **1985**, *94* (4), 632−633.
(21) Tyler, G. Rare earth elements in soil and plant systems - A review. *Plant Soil* **2004**, *267* (1−2), 191−206.
(22) He, P.; He, M.; Zhang, H. State of rare earth elements in the rare earth deposits of Northwest Guizhou, China. *Acta Geochimca* **2018**, *37* (6), 867−874.
(23) Migaszewski, Z. M.; Gałuszka, A. The characteristics, occurrence, and geochemical behavior of rare earth elements in the environment: A review. *Crit. Rev. Environ. Sci. Technol.* **2015**, *45* (5), 429−471.
(24) Leybourne, M. I.; Johannesson, K. H. Rare earth elements (REE) and yttrium in stream waters, stream sediments, and Fe−Mn oxyhydroxides: Fractionation, speciation, and controls over REE + Y patterns in the surface environment. *Geochim. Cosmochim. Acta* **2008**, *72* (24), 5962−5983.
(25) Steinmann, M.; Stille, P. Controls on transport and fractionation of the rare earth elements in stream water of a mixed basaltic−granitic catchment basin (Massif Central, France). *Chem. Geol.* **2008**, *254* (1), 1−18.
(26) Sholkovitz, E. R. The aquatic chemistry of rare earth elements in rivers and estuaries. *Aquat. Geochem.* **1995**, *1* (1), 1−34.
(27) Johannesson, K. H.; Zhou, X. Origin of middle rare earth element enrichments in acid waters of a Canadian High Arctic lake. *Geochim. Cosmochim. Acta* **1999**, *63* (1), 153−165.
(28) Dardenne, S. K.; Schafer, T.; Denecke, T.; Rothe, M. A.; Kim, J. Identification and characterization of sorbed lutetium species on 2-line ferrihydrite by sorption data modeling, TRLFS and EXAFS. *International Journal for Chemical Aspects of Nuclear Science & Technology* **2001**, *89* (7), 469−479.
(29) Nedel, S.; Dideriksen, K.; Christiansen, B. C.; Bovet, N.; Stipp, S. L. Uptake and release of cerium during Fe-oxide formation and transformation in Fe(II) solutions. *Environ. Sci. Technol.* **2010**, *44* (12), 4493−4498.
(30) Nakada, R.; Takahashi, Y.; Tanimizu, M. Isotopic and speciation study on cerium during its solid-water;distribution with implication for Ce stable isotope as a paleo-redox proxy. *Geochim. Cosmochim. Acta* **2013**, *103* (103), 49−62.
(31) Riley, E.; Dutrizac, J. E. The behaviour of the rare earth elements during the precipitation of ferrihydrite from sulphate media. *Hydrometallurgy* **2017**, *172*, 69−78.
(32) Dutrizac, J. E. The behaviour of the rare earths during the precipitation of sodium, potassium and lead jarosites. *Hydrometallurgy* **2004**, *73* (1), 11−30.
(33) Hanchar, J. M.; Westrenen, W. V. Rare earth element behavior in zircon-melt systems. *Elements* **2007**, *3* (1), 37−42.
(34) Quinn, K. A.; Byrne, R. H.; Johan, S. Sorption of yttrium and rare earth elements by amorphous ferric hydroxide: influence of temperature. *Environ. Sci. Technol.* **2007**, *41* (2), 541−546.
(35) Thomas, J. B.; Bodnar, R. J.; Shimizu, N.; Sinha, A. K. Determination of zircon/melt trace element partition coefficients from SIMS analysis of melt inclusions in zircon. *Geochim. Cosmochim. Acta* **2002**, *66* (16), 2887−2901.
(36) Semhi, K.; Abdalla, O. A. E.; Khirbash, S.; Khan, T.; Asaidi, S.; Farooq, S. Mobility of rare earth elements in the system soils−plants−groundwaters: A case study of an arid area (Oman). *Arab Journal of Geosciences* **2009**, *2* (2), 143−150.
(37) Fei, Y.; Hua, J.; Liu, C.; Li, F.; Zhu, Z.; Xiao, T.; Chen, M.; Gao, T.; Wei, Z.; Hao, L. Aqueous Fe(II)-induced phase transformation of ferrihydrite coupled adsorption/immobilization of rare earth elements. *Minerals* **2018**, *8* (8), 357−369.
(38) Das, S.; Hendry, M. J.; Essilfiedughan, J. Effects of adsorbed arsenate on the rate of transformation of 2-line ferrihydrite at pH 10. *Environ. Sci. Technol.* **2011**, *45* (13), 5557−5563.
(39) De La Torre, A. G.; Bruque, S.; Aranda, M. A. G. Rietveld quantitative amorphous content analysis. *J. Appl. Crystallogr.* **2001**, *34* (2), 196−202.
(40) Liu, C. S.; Wang, Y. K.; Li, F. B.; Chen, M. J.; Zhai, G. S.; Tao, L.; Liu, C. P. Influence of geochemical properties and land-use types on the microbial reduction of Fe(III) in subtropical soils. *Environmental Science Processes & Impacts* **2014**, *16* (8), 1938−1947.
(41) Frierdich, A. J.; Catalano, J. G. Controls on Fe(II)-Activated Trace Element Release from Goethite and Hematite. *Environ. Sci. Technol.* **2012**, *46* (3), 1519−1526.
(42) Notini, L.; Latta, D. E.; Neumann, A.; Pearce, C. I.; Sassi, M.; N'Diaye, A. T.; Rosso, K. M.; Scherer, M. M. The role of defects in Fe(II)−goethite electron transfer. *Environ. Sci. Technol.* **2018**, *52* (5), 2751−2759.
(43) Tamura, H.; Goto, K.; Yotsuyanagi, T.; Nagayama, M. Spectrophotometric determination of iron(II) with 1,10-phenanthroline in the presence of large amounts of iron(III). *Talanta* **1974**, *21* (4), 314−318.
(44) Handler, R. M.; Beard, B. L.; Johnson, C. M.; Scherer, M. M. Atom exchange between aqueous Fe(II) and goethite: An Fe isotope tracer study. *Environ. Sci. Technol.* **2009**, *43* (4), 1102−1107.
(45) Handler, R. M.; Frierdich, A. J.; Johnson, C. M.; Rosso, K. M.; Beard, B. L.; Wang, C.; Latta, D. E.; Neumann, A.; Pasakarnis, T.; Premaratne, W. A. Fe(II)-catalyzed recrystallization of goethite revisited. *Environ. Sci. Technol.* **2014**, *48* (19), 11302−11311.
(46) Gorski, C. A.; Fantle, M. S. Stable mineral recrystallization in low temperature aqueous systems: A critical review. *Geochim. Cosmochim. Acta* **2017**, *198*, 439−465.
(47) Neumann, A.; Wu, L.; Li, W.; Beard, B. L.; Johnson, C. M.; Rosso, K. M.; Frierdich, A. J.; Scherer, M. M. Atom exchange between aqueous Fe(II) and structural Fe in clay minerals. *Environ. Sci. Technol.* **2015**, *49* (5), 2786−2795.
(48) ThomasArrigo, L. K.; Mikutta, C.; Byrne, J.; Kappler, A.; Kretzschmar, R. Iron(II)-Catalyzed Iron Atom Exchange and Mineralogical Changes in Iron-rich Organic Freshwater Flocs: An Iron Isotope Tracer Study. *Environ. Sci. Technol.* **2017**, *51* (12), 6897−6907.
(49) Karthikeyan, K.; Elliott, H.; Cannon, F. Adsorption and coprecipitation of copper with the hydrous oxides of iron and aluminum. *Environ. Sci. Technol.* **1997**, *31* (10), 2721−2725.
(50) Kim, M. J. A study on the adsorption characteristics of cadmium and zinc onto acidic and alkaline soils. *Environ. Earth Sci.* **2014**, *72* (10), 3981−3990.
(51) Hoffmann, M.; Christian, M.; Ruben, K. Arsenite binding to sulfhydryl groups in the absence and presence of ferrihydrite: a model study. *Environ. Sci. Technol.* **2014**, *48* (7), 3822−3831.
(52) Ali, A. M.; Eswaran, P.; Hassan, B. Incorporation of silica into the goethite structure: a microscopic and spectroscopic study. *Acta Geochimca* **2018**, *37* (6), 911−921.
(53) Cumplido, J.; Barron, V.; Torrent, J. Effect of phosphate on the formation of nanophase lepidorcrocite from Fe(II) sulfate. *Clays Clay Miner.* **2000**, *48* (5), 503−510.
(54) Ramesh, A.; Lee, D. J.; Wong, J. W. C. Thermodynamic parameters for adsorption equilibrium of heavy metals and dyes from wastewater with low-cost adsorbents. *J. Colloid Interface Sci.* **2005**, *291*, 588−592.
(55) Lide, D. R. *Standard Thermodynamic Properties of Chemical Substances. CRC Handbook of Chemistry and Physics*, 87th ed.; Taylor and Francis: Boca Raton, FL, 2007.
(56) Latta, D. E.; Gorski, C. A.; Scherer, M. M. Influence of $Fe^{2+}$-catalyzed iron oxide recrystallization on metal cycling. *Biochem. Soc. Trans.* **2012**, *40* (6), 1191−1197.
(57) Yan, W. J.; Liu, H.; Chen, R. F.; Xie, J.; Wei, Y. Dissolution and oriented aggregation: Transformation from lepidocrocite to goethite by the catalysis of aqueous Fe(II). *RSC Adv.* **2015**, *5* (129), 106396−106399.
(58) ThomasArrigo, L. K.; Byrne, J. M.; Kappler, A.; Kretzschmar, R. Impact of organic matter on iron(II)-catalyzed mineral transformations in ferrihydrite-organic Matter coprecipitates. *Environ. Sci. Technol.* **2018**, *52* (21), 12316−12326.
(59) Jones, A. M.; Collins, R. N.; Rose, J.; Waite, T. D. The effect of silica and natural organic matter on the Fe(II)-catalyzed trans-


DOI: 10.1021/acsearthspacechem.8b00201
*ACS Earth Space Chem.* 2019, 3, 895−904

formation and reactivity of Fe(III) minerals. *Geochim. Cosmochim. Acta* **2009**, *73* (15), 4409−4422.
(60) Mikutta, C.; Mikutta, R.; Bonneville, S.; Wagner, F.; Voegelin, A.; Christl, I.; Kretzschmar, R. Synthetic coprecipitates of exopolysaccharides and ferrihydrite. Part 1: Characterization. *Geochim. Cosmochim. Acta* **2008**, *72* (13), 1111−1127.
(61) Sinitsyn, V. A.; Aja, S. U.; Kulik, D. A.; Wood, S. A. Acid-base surface chemistry and sorption of some lanthanides on $K^+$-saturated marblehead Illite: I. Results of an experimental investigation. *Geochim. Cosmochim. Acta* **2000**, *64* (2), 185−194.
(62) Sun, T.; Paige, C. R.; Snodgrass, W. J. The effect of cadmium on the transformation of ferrihydrite into crystalline products at pH 8. *Water, Air, Soil Pollut.* **1996**, *91* (3−4), 307−325.
(63) Karthikeyan, K.; Elliott, H. Surface complexation modeling of copper sorption by hydrous oxides of iron and aluminum. *J. Colloid Interface Sci.* **1999**, *220* (1), 88−95.
(64) Nagano, T. Formation of goethite and hematite from neodymium-containing ferrihydrite suspensions. *Clays Clay Miner.* **1999**, *47* (6), 748−754.
(65) Massey, M. S.; Lezama-Pacheco, J. S.; Michel, F. M.; Fendorf, S. Uranium incorporation into aluminum-substituted ferrihydrite during iron(II)-induced transformation. *Environmental Science: Processes & Impacts* **2014**, *16* (9), 2137−2144.
(66) Dardenne, K.; SchaFer, T.; Lindqvist-Reis, P.; Denecke, M. A.; Plaschke, M.; Rothe, J.; Kim, J. I. Low temperature XAFS investigation on the lutetium binding changes during the 2-line ferrihydrite alteration process. *Environ. Sci. Technol.* **2002**, *36* (23), 5092−5099.
(67) Mcdonough, W. F.; Stosch, H. G.; Ware, N. G. Distribution of titanium and the rare earth elements between peridotitic minerals. *Contrib. Mineral. Petrol.* **1992**, *110* (2−3), 321−328.
(68) Li, P.; Zhun, B.; Wang, X. G.; Liao, P. P.; Wang, G. H.; Wang, L. Z.; Guo, Y. D.; Zhang, W. M. Highly Efficient Interception and Precipitation of Uranium(VI) from Aqueous Solution by Iron-Electrocoagulation Combined with Cooperative Chelation by Organic Ligands. *Environ. Sci. Technol.* **2017**, *51* (24), 14368−14378.
(69) Liu, G. F.; Yu, H. L.; Wang, N.; Jin, R. F.; Wang, J.; Zhou, J. T. Microbial reduction of Ferrihydrite in the presence of reduced Graphene oxide materials: Alteration of Fe(III) reduction rate, biomineralization product and settling behavior. *Chem. Geol.* **2018**, *476*, 272−279.
(70) Hua, J.; Chen, M. J.; Liu, C. S.; Li, F. B.; Long, J.; Long, S. Q.; Lei, J.; Liu, Y. H. Cr release from Cr-substituted goethite during the recrystallization induced by aqueous Fe(II). *Minerals* **2018**, *8* (9), 367−382.
(71) Singh, B.; Sherman, D.; Mosselmans, J.; Gilkes, R.; Wells, M. Incorporation of Cr, Mn and Ni into goethite ($\alpha$-FeOOH): Mechanism from extended X-ray absorption fine structure spectroscopy. *Clay Miner.* **2002**, *37* (4), 639−649.
(72) Owen, A. W.; Armstrong, H. A.; Floyd, J. D. Rare earth element geochemistry of upper Ordovician cherts from the Southern Uplands of Scotland. *Journal of the Geological Society* **1999**, *155*, 191−204.
(73) O'Neill, L. C.; Elliott, B. A.; Kyle, J. R. Mineralogy and crystallization history of a highly differentiated REE-enriched hypabyssal rhyolite: Round Top laccolith, Trans-Pecos, Texas. *Mineral. Petrol.* **2017**, *111* (4), 569−593.



DOI: 10.1021/acsearthspacechem.8b00201
*ACS Earth Space Chem.* 2019, 3, 895−904